# Statistical Characterization of Ultrasonic Additive Manufacturing Ti/Al Composites

**C. D. Hopkins**
Department of Mechanical Engineering,
Ohio State University,
201 West 19th Avenue,
Columbus, OH 43210
e-mail: hopkins.626@osu.edu

**M. J. Dapino**[1]
Department of Mechanical Engineering,
E307 Scott Laboratory,
Ohio State University,
201 West 19th Avenue,
Columbus, OH 43210
e-mail: dapino.1@osu.edu

**S. A. Fernandez**
Center for Biostatistics,
Ohio State University,
2012 Kenny Road,
Columbus, OH 43221
e-mail: fernandez.71@osu.edu

*Ultrasonic additive manufacturing (UAM) is an emerging solid-state fabrication process that can be used for layered creation of solid metal structures. In UAM, ultrasonic energy is used to induce plastic deformation and nascent surface formation at the interface between layers of metal foil, thus creating bonding between the layers. UAM is an inherently stochastic process with a number of unknown facets that can affect the bond quality. In order to take advantage of the unique benefits of UAM, it is necessary to understand the relationship between manufacturing parameters (machine settings) and bond quality by quantifying the mechanical strength of UAM builds. This research identifies the optimum combination of processing parameters, including normal force, oscillation amplitude, weld speed, and number of bilayers for the manufacture of commercially pure, grade 1 titanium + 1100-O aluminum composites. A multifactorial experiment was designed to study the effect of the above factors on the outcome measures ultimate shear strength and ultimate transverse tensile strength. Generalized linear models were used to study the statistical significance of each factor. For a given factor, the operating levels were selected to cover the full range of machine capabilities. Transverse shear and transverse tensile experiments were conducted to quantify the bond strength of the builds. Optimum levels of each parameter were established based on statistical contrast trend analyses. The results from these analyses indicate that high mechanical strength can be achieved with a process window bounded by a 1500 N normal force, 30 $\mu$m oscillation amplitude, about 42 mm/s weld speed, and two bilayers. The effects of each process parameter on bond strength are discussed and explained.*
[DOI: 10.1115/1.4002073]

## 1 Introduction

Ultrasonic additive manufacturing (UAM) or ultrasonic consolidation is a recent manufacturing process that combines principles from ultrasonic welding, layered manufacturing techniques, and subtractive processes to create metal parts with arbitrary shapes and features [1]. UAM is a solid-state welding process that allows joining of metallic materials far below their respective melting temperatures. The locally generated heat due to ultrasonic vibration during the UAM process ranges between 30% and 50% of the melting temperature of the base metal [2]. For this reason, UAM offers unprecedented opportunities to create parts with embedded elements that are sensitive to thermal loading, such as smart materials or electronic components [3,4]. Further, the subtractive stage integrated within the UAM system allows for the simultaneous incorporation of arbitrarily shaped internal features such as cooling channels or designed anisotropies. Finally, UAM has been utilized to embed and join both difficult and dissimilar metals and materials such as Ti, Al, Cu, Mg, and stainless steel alloys.

The UAM process, in which successive layers of metal tape are bonded together, is based on the technology of ultrasonic metal welding. A sonotrode or horn is used to apply a normal force at the interface between two metal work pieces. An ultrasonic transducer drives the transversely vibrating sonotrode, which imparts a motion to the top work piece and creates a relative, frictionlike action at the interface of the two work pieces (Fig. 1). This scrubbing motion causes shear deformations of contacting surface asperities, dispersing interface oxides and bringing clean metal-to-metal contact and adhesion between the faying surfaces [5].

The UAM system is distinct from conventional metal welding systems. As shown in Fig. 2, instead of a spot contact, vibrations generated by a piezoelectric ultrasonic transducer are transmitted into the parts through a rolling horn. The rate of displacement of the horn relative to the build is referred to as the weld speed and is an operator-defined process parameter. The vibrations propagate longitudinally at a frequency of 20 kHz from the transducer to the horn through tuned waveguides. The amplitude of these vibrations is considered a process parameter that can be adjusted. Normal force can be adjusted and applied to the vibrating horn as it rolls along the work piece, and the vibrations transmitted to the weld interface cause a solid-state bond between the parts. Current UAM systems achieve the most effective bonding on thin metal layers of approximately 152 $\mu$m thickness. The UAM system employs either an automated feed mechanism for allowing successive layers of metal tapes, drawn from a continuous spool, or thin sheets to be bonded together for creating larger bulk builds. A subtractive computed numerically controlled (CNC) machining stage is also fully automatic and integrated within the UAM system [5].

Several studies have related bond quality to manufacturing parameters (machine settings), mainly normal force, oscillation amplitude, and weld speed. Most of these studies focused on 3003-H18 aluminum as the matrix material and assessed the bond quality by reporting either peel strength data or linear weld density measurements [2,6,7]. Currently, neither of these tests can be used as a direct comparison to commonly used material properties. Further, studies focused on Ti/Al composites have not been reported. In UAM, the force, oscillation amplitude, and weld speed can be adjusted over a broad range, but it is unclear how these parameters and combinations of them affect the process and resulting build strength. The main objective of this research is to characterize the dependence of mechanical properties on process

[1]Corresponding author.

Contributed by the Materials Division of ASME for publication in the JOURNAL OF ENGINEERING MATERIALS AND TECHNOLOGY. Manuscript received January 16, 2010; final manuscript received June 18, 2010; published online September 29, 2010. Assoc. Editor: Hussein Zbib.

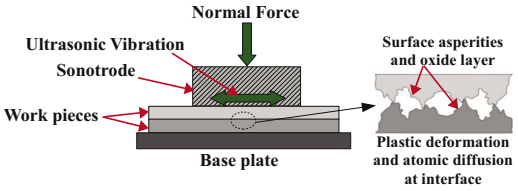


**Fig. 1 Schematic representation of ultrasonic metal welding and detailed view of the weld zone (inset)**

parameters for UAM composites comprising Ti/Al bilayers. Statistical models were used to account for the stochastic nature of the UAM process. Trends in the response variable data were detected and statistically verified. Titanium-aluminum builds were chosen to be investigated because of their relevance in high strength composite applications. Finally, mechanical testing procedures were developed for this research which may be applicable to future UAM mechanical strength investigations.

The present study uses a design of experiment (DOE) approach in order to fully explore the effects of normal force, oscillation amplitude, weld speed, and number of bilayers on the ultimate shear strength (USS) and ultimate transverse tensile strength (UTTS) of UAM Ti/Al builds. A bilayer consists of one titanium layer on top of one aluminum layer without any welding in between, as shown in Fig. 3. The parts are built by successively welding one bilayer onto another.

## 2 Experimental Methods

**2.1 Sample Fabrication and Statistical Procedures.** The materials used in this research were 127 $\mu$m thick sheets of commercially pure, annealed grade 1 titanium and 1100-O aluminum. All samples were built by Solidica, Inc., Ann Arbor, MI and were 19 mm high by 63.5 mm wide and 292 mm long. The samples were all built at a baseplate preheat temperature of 150°C and

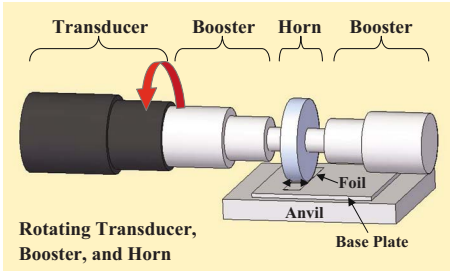


**Fig. 2 Diagram of UAM system where successive layers of metal tape are bonded together for creating bulk metallic parts**

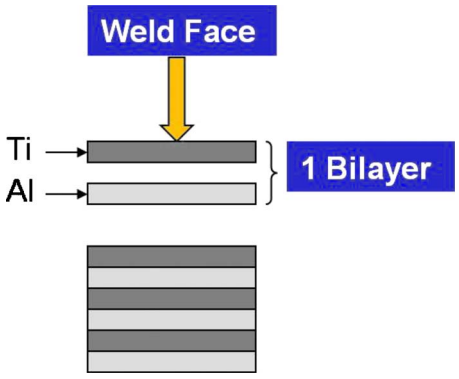


**Fig. 3 Schematic representation of Ti/Al bilayers**

**Table 1 Process parameters and levels used in this study**

| Parameter | Level 1 | Level 2 | Level 3 | Level 4 |
|---|---|---|---|---|
| Normal force (N) | 500 | 1000 | 1500 | 2000 |
| Oscillation amplitude ($\mu$m) | 15 | 20 | 25 | 30 |
| Weld speed[a] (in./min) | 50 (21 mm/s) | 100 (42 mm/s) | 150 (64 mm/s) | 200 (85 mm/s) |
| No. of bilayers | 2 | 4 | 6 | 8 |

[a]The default machine input unit is in/min. Reported values in mm/s are rounded off to nearest integer.

were subjected to a post-process heat treatment of 4 h at 480°C followed by furnace cooling. The samples were then machined to the geometries needed for testing.

A Taguchi L16 orthogonal array was employed for the experimental design. The Taguchi array is a statistically robust design that reduces the number of treatment combinations from 256 to 16 for a design consisting of four parameters at four levels each [8]. The process parameters and their corresponding levels are shown in Table 1. The levels for each of the manufacturing parameters were selected because they represent an even distribution across the range of machine operation limits for each setting.

Table 2 shows the Taguchi orthogonal array with the coded parameter levels. Generalized linear models with four main effects (normal force, amplitude, weld speed, and number of bilayers) were used to study trends in each outcome variable (USS and UTTS). The linear model equation and model assumptions utilized are

$$Y_{ijklt} = \mu + \alpha_i + \beta_j + \gamma_k + \delta_l + \epsilon_{ijklt}$$

$$\epsilon_{ijklt} \sim i.i.d.\ \ N(0,\sigma^2) \qquad (1)$$

$$i = j = k = l = t = 1,2,3,4$$

This linear model describes the dependence of the response variable (USS or UTTS), $Y_{ijklt}$, upon the levels of the treatment factors [9]. In Eq. (1), $\mu$ denotes the overall mean of the response variable. The effects of each of the process parameters on the mean response are represented by $\alpha_i$, $\beta_j$, $\gamma_k$, and $\delta_l$, where $\alpha_i$ is the effect of normal force at the $i$th level on the response while the other three factors are fixed. Similarly, $\beta_j$, $\gamma_k$, and $\delta_l$ represent the effects of amplitude, weld speed, and number of bilayers at the $j$th, $k$th, and $l$th levels, respectively, while the other factors are fixed. The error variable, $\epsilon_{ijklt}$, is a random variable with zero mean, which denotes any nuisance variation in the response. In

**Table 2 Coded Taguchi L16 orthogonal array**

| Treatment combination | Normal force | Amplitude | Weld speed | No. of bilayers |
|---|---|---|---|---|
| 1 | 1 | 1 | 1 | 1 |
| 2 | 1 | 2 | 2 | 2 |
| 3 | 1 | 3 | 3 | 3 |
| 4 | 1 | 4 | 4 | 4 |
| 5 | 2 | 1 | 2 | 3 |
| 6 | 2 | 2 | 1 | 4 |
| 7 | 2 | 3 | 4 | 1 |
| 8 | 2 | 4 | 3 | 2 |
| 9 | 3 | 1 | 3 | 4 |
| 10 | 3 | 2 | 4 | 3 |
| 11 | 3 | 3 | 1 | 2 |
| 12 | 3 | 4 | 2 | 1 |
| 13 | 4 | 1 | 4 | 2 |
| 14 | 4 | 2 | 3 | 1 |
| 15 | 4 | 3 | 2 | 4 |
| 16 | 4 | 4 | 1 | 3 |

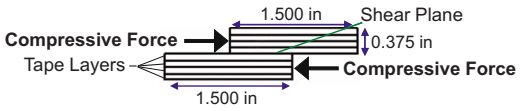


**Fig. 4 Loading scheme and tape diagram of shear specimens (not to scale)**

this model, it is assumed that the error variables are independent and that they have a normal distribution with zero mean and constant variance.

Several samples could not be built due to delamination during manufacture or machining. As a result of the limited sample size, and for simplicity, the models were reduced to include combinations of two main effects per model (bivariate models).

Four shear and four transverse tensile samples were created and tested per experimental run. All mechanical tests were run on a 20 kip (89 kN) interlaken load frame fitted with a ±5000 lb (22.2 kN) load cell and integrated linear variable differential transformer (LVDT). The load frame was connected to an MTS 458.20 micro console controller that was coupled to a data acquisition system comprising a Data Physics dynamic signal analyzer and a PC. All tests were run under displacement control with a ramp and hold input program. Because the LVDT measures the deflection of the test frame actuator, all displacement data include displacement generated within the load train as well as the specimen. Consequently, the resulting force-displacement plots can only be used to determine if a given sample failed in brittle or ductile mode through qualitative analyses. Further, these data cannot be used to calculate specimen strain or related properties such as the elastic modulus. The statistical analyses were performed using SAS 9.1 statistical software [10].

**2.2 Transverse Shear Testing.** UAM shear specimens were built based on the ASTM standard test method for lap shear strength of sealants (ASTM C 961-06). The specimens were designed such that a tape layer was oriented along the shear plane, as shown in Fig. 4. The samples were received as $2.500 \times 0.675 \times 0.750$ in.$^3$ ($63.50 \times 17.15 \times 19.05$ mm$^3$) rectangular prisms, which were then machined down to final dimensions. The samples were tested by placing them in a shear jig where one leg is supported and the other leg is loaded from the top. Figure 5 shows a sample in the shear jig just prior to being tested in the load frame. Loading was applied until sample failure while measuring force and hydraulic ram displacement.

**2.3 Transverse Tensile Testing.** UAM transverse tensile specimens were built such that the tape layers were perpendicular to the applied axial loading (Fig. 6). Since this geometry and test method does not adhere to known standards, control tests were run with a solid wrought piece of 3003 aluminum. The test does not bias the ultimate tensile strength and is repeatable. Therefore, the geometry shown was used for the transverse tensile testing of the Ti/Al samples in this research. The samples were received as $0.375 \times 0.375 \times 0.750$ in.$^3$ ($9.53 \times 9.53 \times 19.05$ mm$^3$) rectangular prisms, which were then machined down to final dimensions. Tensile strength of the bonding between the layers was tested by placing the samples into specially designed grips. Figure 7 shows the configuration of the grips and the samples. The samples were axially loaded until failure while the force and the hydraulic ram displacement were recorded.

**2.4 Micrograph Preparation.** After mechanical testing, the bond interface of selected samples was examined at a microscopic level to determine if there is a correlation between macroscopic mechanical strength and microstructure in UAM Ti/Al composites. Samples were cross sectioned (perpendicular to weld direction) and polished following standard metallographic procedures. Observations were conducted on as-polished samples using an optical microscope under various magnifications.

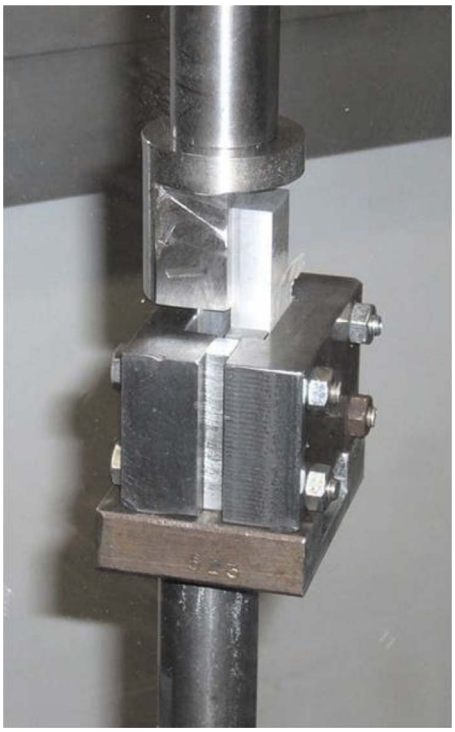

**Fig. 5 UAM shear specimen strength testing set-up**

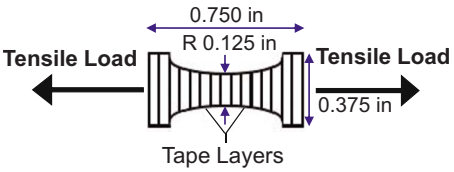


**Fig. 6 Loading scheme and tape diagram of transverse tensile specimens (not to scale)**

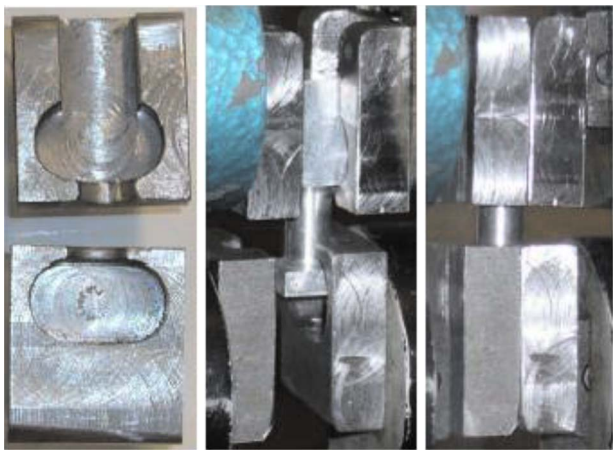

**Fig. 7 (Left to right) transverse tensile sample grips, grips installed in jaws, and sample in grips prior to testing**

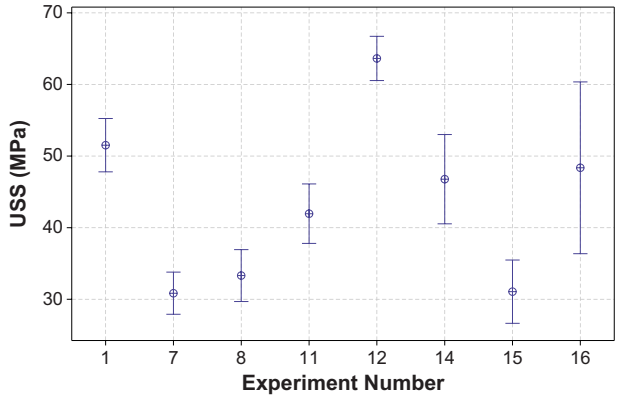


**Fig. 8 Interval plot showing USS for shear experiments—bars are one standard error from mean (crosshair)**

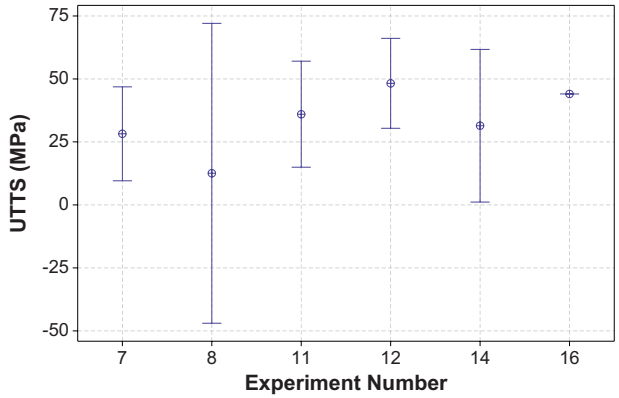


**Fig. 9 Interval plot showing UTTS for transverse tensile experiments—bars are one standard error from mean (crosshair)**

## 3 Results

**3.1 Mechanical Test Results.** The breaking force varied considerably between samples within individual experiments and between experiments. Figures 8 and 9, respectively, show the USS and UTTS averages over the sample replicates and the standard error. The standard error is defined as the standard deviation over the square root of the total number of samples studied. The breaking force was measured at the time when the specimen underwent complete failure, right before the force decreased significantly. There are only 8 of 16 experimental runs that could be tested for shear and only 6 of 16 experimental runs that could be tested for transverse tension.

Surface plots of the response variables are shown in Figs. 10 and 11. These measurements indicate that attainment of the highest USS and UTTS requires a combined selection of 1500 N normal force, 30 $\mu$m or more amplitude, 42–64 mm/s weld speed, and only two bilayers. Moreover, there is no likely interaction between the parameters at these levels because the levels that produce the highest response are the same between plots of varying combinations of parameters.

**3.2 Statistical Analysis of Mechanical Strength Tests.** The USS and UTTS data were analyzed statistically by fitting generalized linear models. The type I error probability selected for this experiment is $\alpha=0.05$ for testing each of the model parameters. The $\alpha$ level is the threshold probability of a false positive (type I error), that is, rejecting the null hypothesis when it is true. The $p$ value represents the probability of obtaining a test at least as extreme as the one observed, assuming that the null hypothesis of no trend or no effect is true. The lower the $p$ value, the stronger the evidence against the null hypothesis; when $p<\alpha$, the null hypothesis is rejected in favor of the alternative hypothesis (there is a trend or an effect).

The results from the bivariate models are shown in Table 3 for the USS data and Table 4 for the UTTS data. The results for the USS data show that the two best models (highest $R^2$ values) are the ones including normal force and amplitude ($R^2=0.6144$) and weld speed and number of bilayers ($R^2=0.6892$). In addition,

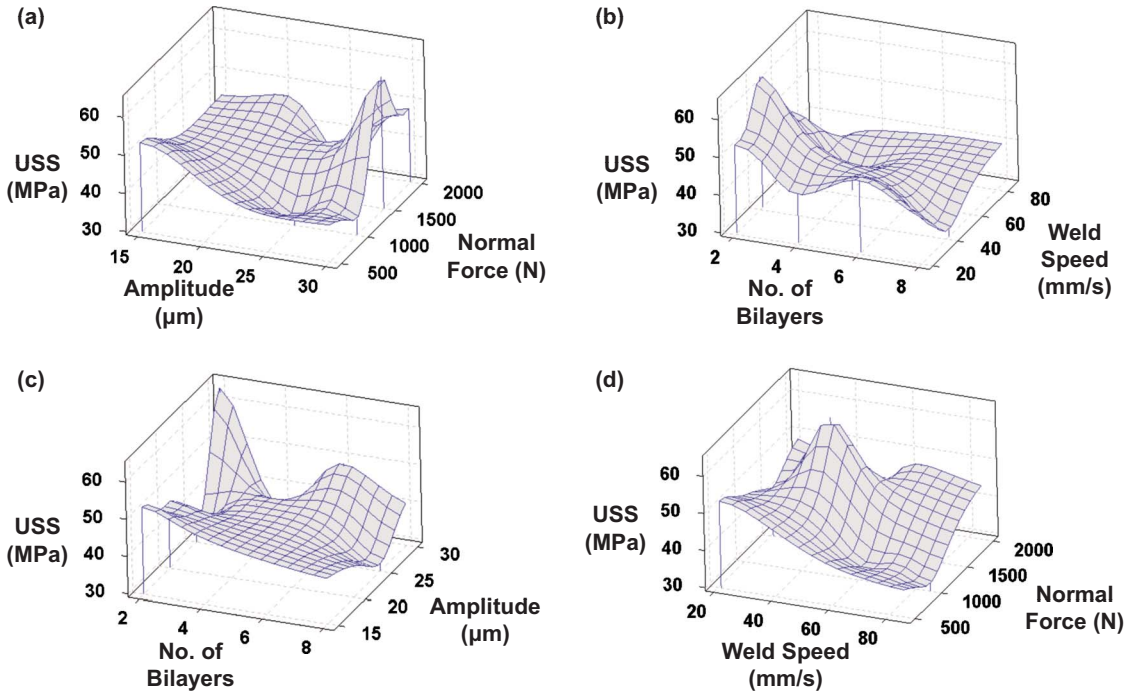


**Fig. 10 Surface plots of USS as a function of (*a*) normal force and amplitude, (*b*) weld speed and no. of bilayers, (*c*) amplitude and no. of bilayers, and (*d*) normal force and weld speed**

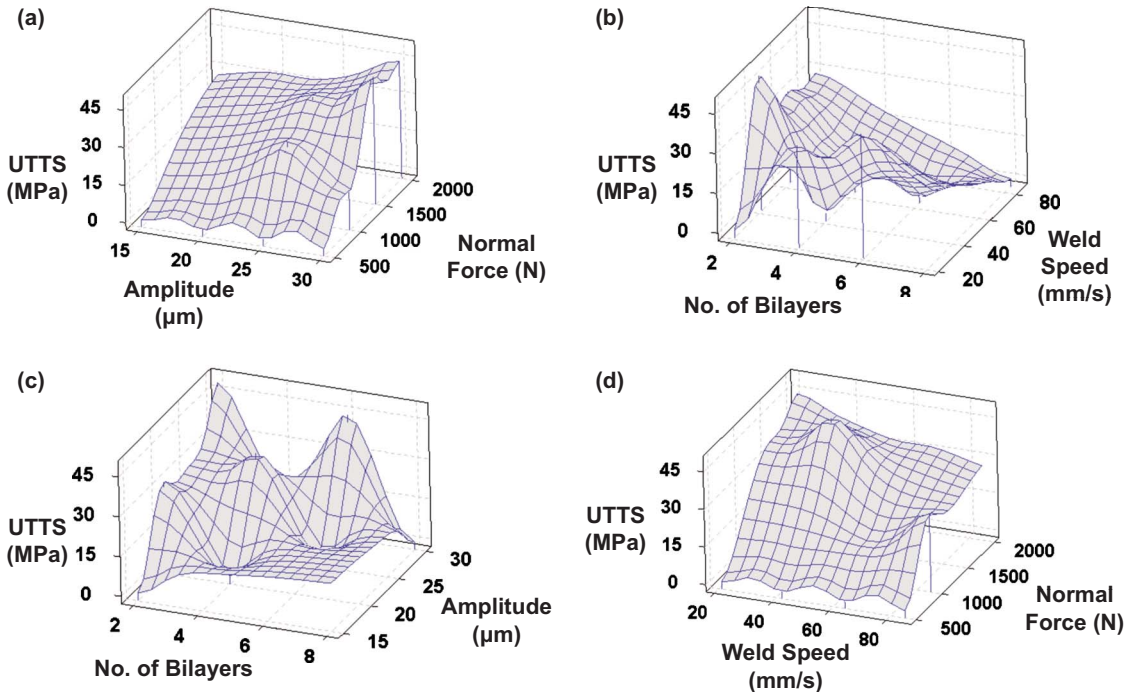


**Fig. 11 Surface plot illustrating UTTS as influenced by (*a*) normal force and amplitude, (*b*) weld speed and no. of bilayers, (*c*) amplitude and no. of bilayers, and (*d*) normal force and weld speed**

these two models have $p < \alpha$ for each of the two factors. The $R^2$ value represents the proportion of the total variability in the response variable explained by the model. Table 4 shows that the two best models for UTTS are the ones including weld speed and number of bilayers ($R^2=0.7394$) and normal force and weld speed ($R^2=0.7394$). Therefore, 74% of the variability in UTTS is explained by either bivariate model. For these two models, weld speed is significant when combined with number of bilayers but not when combined with normal force. This result is likely an artifact of the limited UTTS data as it is not consistent with the results from the USS data. The model fits correlate well with the surface measurements shown in Figs. 10 and 11.

In addition to understanding the significance of the parameters we examined trends in the data by fitting univariate models. Figures 12 and 13 show USS and UTTS measurements, respectively, for each parameter at each level averaged over all other levels and parameters. The plots show polynomial functions that best fit the data. These functions are shown in Table 5 along with their corresponding $R^2$ values, which provide a quantitative measure of the ability of the regression lines to accurately describe the data

**Table 3 ANOVA table for two-factor generalized linear models for USS data**

| Source of variation | Degrees of freedom | Type III sum of squares | Mean square | F-ratio | *p* value | $R^2$-value |
|---|---|---|---|---|---|---|
| Normal force | 2 | 1769.5688 | 884.7844 | 9.9 | 0.0010 | 0.6144 |
| Amplitude | 2 | 1121.78838 | 560.8942 | 6.27 | 0.0077 | |
| Weld speed | 3 | 2014.4929 | 671.4977 | 8.85 | 0.0007 | 0.6892 |
| No. of bilayers | 3 | 2305.1676 | 768.3892 | 10.13 | 0.0003 | |
| Amplitude | 3 | 442.7438 | 147.5813 | 0.93 | 0.4452 | 0.3502 |
| No. of bilayers | 3 | 544.4273 | 181.4758 | 1.14 | 0.3567 | |
| Normal force | 3 | 1178.2318 | 392.7439 | 2.91 | 0.0615 | 0.4461 |
| Weld speed | 3 | 341.4602 | 113.8201 | 0.84 | 0.4877 | |

**Table 4 ANOVA table for two-factor generalized linear models for UTTS data**

| Source of variation | Degrees of freedom | Type III sum of squares | Mean square | F-ratio | *p* value | $R^2$-value |
|---|---|---|---|---|---|---|
| Normal force | 2 | 1290.3617 | 645.1808 | 5.20 | 0.0283 | 0.5311 |
| Amplitude | 2 | 107.7116 | 53.8558 | 0.43 | 0.6593 | |
| Weld speed | 3 | 1453.3942 | 484.4647 | 6.33 | 0.0135 | 0.7394 |
| No. of bilayers | 2 | 404.8907 | 202.4453 | 2.64 | 0.1249 | |
| Amplitude | 2 | 118.9572 | 59.4786 | 0.29 | 0.7515 | 0.2348 |
| No. of bilayers | 2 | 506.7569 | 253.3784 | 1.25 | 0.3271 | |
| Normal force | 2 | 404.8907 | 202.4453 | 2.64 | 0.1249 | 0.7394 |
| Weld speed | 3 | 658.5437 | 219.5146 | 2.87 | 0.0962 | |

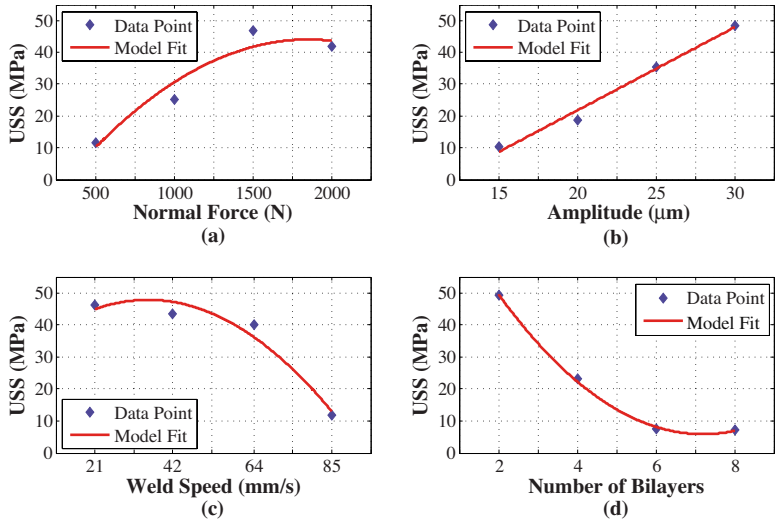


**Fig. 12 Deviation in average USS as a function of selected levels for each parameter: (*a*) USS versus normal force, (*b*) USS versus amplitude, (*c*) USS versus weld speed, and (*d*) USS versus number of bilayers**

within the measured range. Most of the $R^2$ values are higher than 0.96, which indicates strong linear associations with the response variables. The fitted linear models with $R^2 < 0.96$ (normal force for the USS data and normal force and weld speed for the UTTS data) are good estimates of the observed trend, but not all the variability in the response variables is explained by these models.

Linear trend contrasts were tested at a 0.01 significance level. Table 6 shows the results of this analysis; there is a straight-line relationship between the USS and the UTTS data and all the four parameters (all parameters have small $p$ values). Figures 12 and 13 illustrate that there is an increasing straight line in the cases of normal force and amplitude and a decreasing trend in the cases of weld speed and number of bilayers. For the USS, the trend contrasts demonstrate that amplitude has a slight quadratic trend ($p = 0.0059$), most likely due to the influence of the response at level 2. The normal force, weld speed, and number of bilayers for the USS data exhibit significant quadratic trends. For the UTTS, there is no significant quadratic trend present in the amplitude and weld speed data ($p = 0.6786$ and $p = 0.1732$, respectively). Both normal force and number of bilayers show a significant quadratic trend.

**3.3 Micrographs of Bond Interface.** The samples chosen for microstructural investigation correspond to experiment 7, sample 3 (sample 7-3) and experiment 12, sample 1 (sample 12-1). These specimens were selected because sample 7–3 exhibits relatively low USS and UTTS (28.67 MPa and 24.89 MPa, respectively) and sample 12-1 exhibits relatively high USS and UTTS (61.22 MPa and 32.79 MPa, respectively). We compare the microstructures of these two samples and seek to investigate differences between them that may explain the difference in mechanical strengths. Figures 14 and 15 are typical images of the tape layers at 100× magnification for samples 7-3 and 12-1, respectively.

Both of the samples were built using two bilayers with the titanium layer in contact with the welding horn. Therefore, every four layers (aluminum on the bottom and titanium on the top), the horn is in contact with the top titanium layer. Previous research has shown that there is a significant increase in roughness on the surfaces in contact with the horn during the UAM process [11]. This can be seen in Fig. 14 but it is noted that while both samples were built using two bilayers, sample 7-3 had 1000 N normal force, 25 $\mu$m amplitude, and 85 mm/s weld speed whereas

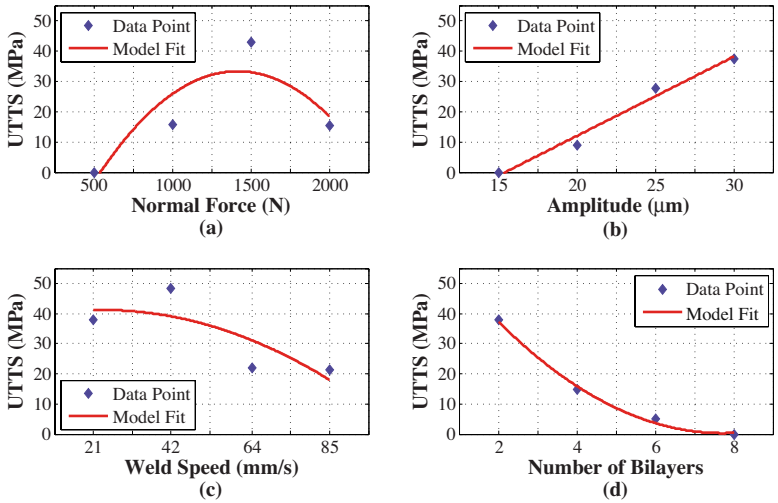


**Fig. 13 Deviation in average UTTS as a function of selected levels for each parameter: (*a*) UTTS versus normal force, (*b*) UTTS versus amplitude, (*c*) UTTS versus weld speed, and (*d*) UTTS versus number of bilayers**

**Table 5 Equations of the linear model fits for trends in USS and UTTS data**

| Mechanical response | Parameter | Model fit equation | $R^2$-value |
|---|---|---|---|
| USS | Normal force | $y=-4.613x^2+34.316x-19.797$ | 0.9202 |
| | Amplitude | $y=13.058x-4.367$ | 0.9846 |
| | Weld speed | $y=-6.404x^2+21.327x+30.062$ | 0.9616 |
| | No. of bilayers | $y=6.453x^2-46.459x+89.503$ | 0.9989 |
| UTTS | Normal force | $y=-10.850x^2+61.569x-54.053$ | 0.7685 |
| | Amplitude | $y=-40.413x+2.618$ | 0.9808 |
| | Weld speed | $y=-2.769x^2$ 6.168$x$+37.700 | 0.6289 |
| | No. of bilayers | $y=67.922x^2-17.518x+1.135$ | 0.9961 |

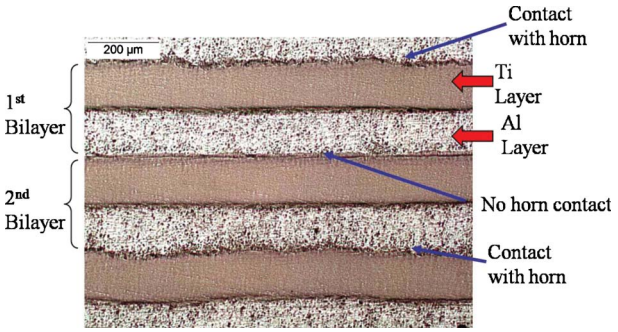


**Fig. 15 UAM built Ti/Al sample 12-1 at 100x magnification**

sample 12-1 had 1500 N normal force, 30 $\mu$m amplitude, and 42 mm/s weld speed. Consequently, the layers that were welded in sample 7-3 are not expected to be as rough as layers welded in sample 12-1.

Figures 16 and 17 show closer views of the two samples. Similar observations can be made for both samples. The area labeled region I shows foreign particles distributed throughout the aluminum tape layer. Evaluation of these particles and the immediate surrounding areas using a scanning electron microscope (SEM), an energy dispersive X-ray spectroscope (EDX), and a backscatter electron SEM show that these particles are composed of silicon originating from the SiC grit disks used for polishing the samples. The EDX results for one of the particles tested are shown in Fig. 18. The harder titanium breaks off pieces of the silicon disk during polishing, and the ensuing particles become lodged into the much softer aluminum layer. The entire interface was checked using EDX, and it was found that the post-process heat treatment did not induce intermetallic compounds. In region II, the aluminum layer appears to have smeared into the crevasses of the titanium build below it. Finally, the lack of typical voids at the interface is quite noticeable and is explained in Sec. 4.4.

## 4 Discussion

**4.1 Mechanical Strength of Transverse Shear Specimens.** Most of the samples exhibited a predominantly linear relationship between force and displacement and failed in a macro-level brittle fracture mode. Additionally, there was considerable variation in USS with standard deviations ranging from 5.10 MPa to 20.76 MPa between experiments. For experiment 16, the average USS was 32.66 MPa with a standard deviation of 20.76 MPa, which is 63% of the average value. This result highlights the inconsistency of the USS for Ti/Al shear samples made by UAM.

Experiment 12 produced the highest strengths with an average of 63.63 MPa and a standard deviation of 6.27 MPa. The USS for a sample made under the parameters of experiment 12 was about

**Table 6 *P* values for trend contrasts in USS and UTTS data as a function of UAM process parameters**

| Mechanical response | Parameter | Straight-line trend $p$ value | Quadratic trend $p$ value |
|---|---|---|---|
| USS | Normal force | <0.0001 | 0.0010 |
| UTTS | | 0.0017 | 0.0002 |
| USS | Amplitude | <0.0001 | 0.0059 |
| UTTS | | <0.0001 | 0.6786 |
| USS | Weld speed | <0.0001 | <0.0001 |
| UTTS | | 0.0006 | 0.1732 |
| USS | No. of bilayers | <0.0001 | <0.0001 |
| UTTS | | <0.0001 | <0.0001 |

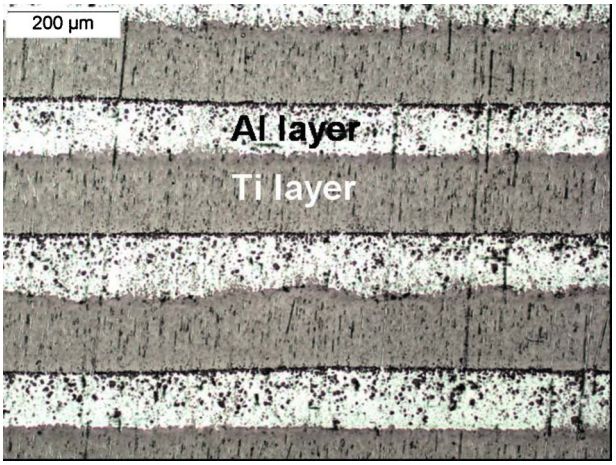


**Fig. 14 UAM built Ti/Al sample 7-3 at 100x magnification**

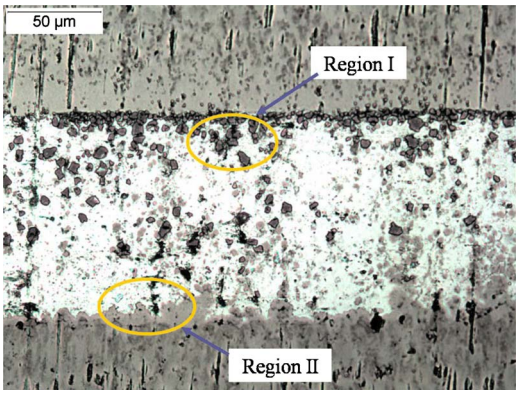


**Fig. 16 UAM built Ti/Al sample 7-3 at 400x magnification**

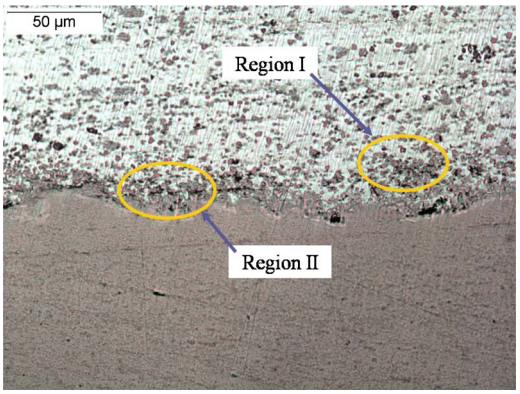


**Fig. 17 UAM built Ti/Al sample 12-1 at 400x magnification**

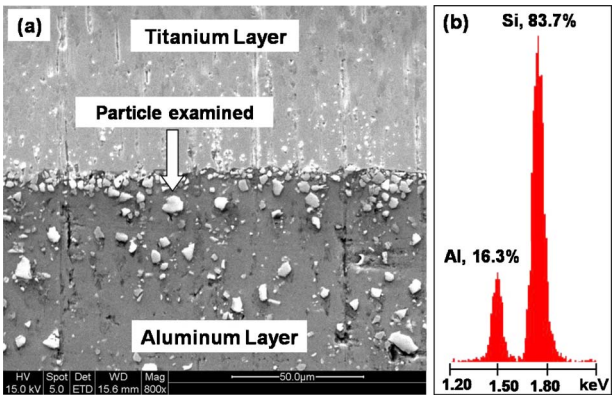


**Fig. 18** (*a*) **Location of one of the foreign particles examined and** (*b*) **the particles are composed of silicon originating from the SiC grit disks used for polishing**

the same as the USS of solid 1100-O aluminum (62 MPa). For samples made under optimal welding parameters, the aluminum layer is expected to fail at about the same stress as the bonds, causing a spike in the stress of the titanium layers, leading to a complete failure of the build. While this experiment produced strengths close to the failure strength of one of the parent materials, most of the other experiments had strengths up to 50% less than solid 1100-O aluminum.

**4.2 Mechanical Strength of Transverse Tensile Specimens.** All samples exhibited a predominantly linear relationship between force and displacement and failed in a macro-level brittle fracture mode. The samples failed at a single weld interface and produced two separate pieces. Significant deviation in UTTS was observed; standard deviations ranged from 3.37 MPa to 11.22 MPa between experiments. For experiment 8, the average UTTS was 12.55 MPa with a standard deviation of 6.62 MPa, which is 53% of the average value. Similar to the shear tests, experiment 12 produced the highest strengths with an average of 48.25 MPa and a standard deviation of 11.22 MPa. This is only about 40% of the ultimate tensile strength of solid 1100-O aluminum. These results show that UTTS is more consistent than USS, although UAM samples are weaker in the transverse tensile direction than in shear.

### 4.3 Effects of Manufacturing Parameters

*4.3.1 Normal Force*. It can be seen from Figs. 12(*a*) and 13(*a*) that USS and UTTS exhibit a maximum near 1500 N and a relatively linear dependence below this force value. This type of dependence is consistent with results found by Kong et al. [2], Yang et al. [12], and Janaki Ram et al. [13] for UAM builds. While the material tested in those studies was 3003 aluminum, it can be assumed that the same mechanism causing this behavior is present in UAM Ti/Al composites. Although the exact nature of this mechanism is not known, we speculate that too high of a normal force can result in excessive interfacial stresses, causing breakage of previously formed bonds. Second, the increase in normal force leads to an increase in the welding horn's oscillatory force needed to maintain a given frequency. The high normal force prevents the horn from oscillating at the desired amplitude, thereby reducing the effectiveness of the UAM process [12].

*4.3.2 Oscillation Amplitude*. Unlike normal force, oscillation amplitude linearly affects the USS and UTTS across the chosen levels, as shown in Figs. 12(*b*) and 13(*b*). As the oscillation amplitude increases, the relative USS and UTTS also increase. High vibration amplitudes result from higher vibratory energy and higher associated shear forces at the weld interface. This leads to better removal of any oxide films or other contaminants on the surface of the layers. The break-up of these surface impurities permits better metal-to-metal contact of the faying surfaces, which allows for elastic-plastic deformation and atomic diffusion to take place at the interface [2].

*4.3.3 Weld Speed*. As shown in Fig. 12(*c*), the USS slightly declined when the welding speed increased from 21–64 mm/s and decreased abruptly beyond 64 mm/s. Based on the results of this experiment, a slower weld speed produces a higher USS in Ti/Al specimens. Figure 13(*c*) shows that the UTTS abruptly increased from 40 MPa to almost 50 MPa between 21 mm/s and 42 mm/s and then decreased drastically at speeds of 64 mm/s and 85 mm/s. This trend is slightly different from the one found for the shear tests. The spike in the UTTS at 42 mm/s occurs because the values used for calculating that point were all from the same treatment combination (experiment 12), which produced very high tensile strengths because of the other parameter settings. Overall, for the weld speeds used in this experiment, a slower weld speed produces a higher UTTS in UAM Ti/Al specimens. Welding speed determines the amount of energy input per unit length. The slower the welding horn moves across the build plate, the more time is allowed for contact between the oscillating horn and the material, thereby increasing the total energy put into the build. Conversely, by increasing the welding speed, the horn resident time reduces, leading to inadequate oxide layer removal and less plastic deformation at the interface [2,12].

*4.3.4 Number of Bilayers*. The number of bilayers that are stacked between welds has a significant effect on the strength of the build. The data in Figs. 12(*d*) and 13(*d*) show that there is a negative linear trend of the USS and UTTS as the number of bilayers is increased. For a greater number of bilayers, the same energy imparted by the welding horn needs to be dispersed through a larger volume of material. In addition, as the height of the build increases, the part becomes more compliant, thus resulting in greater deflection of the part. In turn, there is an increase in the relative motion between the part and the horn, which means that energy is being used to deflect the part, so there is less energy available for the scrubbing action of the horn on the material. This experiment shows that for a given available ultrasonic energy, the fewer the bilayers, the better the chance of building a solid part because of superior bonding between layers.

**4.4 Examination of Bond Interface Microstructure.** It has been shown that in ultrasonic welding of two dissimilar metals, there is extensive mechanical interlocking and deformation; the softer of the two materials flows around the surface topography of the harder material [14]. Because aluminum is much softer than titanium, the asperities on the titanium surface do not undergo sufficient deformation to allow for nascent surface creation. The aluminum tape simply conforms to the shape of the titanium faying surface, which prevents solid-state metallurgical bonding from occurring. As a result, the strength of the build is based mainly on mechanical interlocking of the materials. The span of strengths exhibited by the samples in this DOE is attributed to the amount and severity of roughness imposed by the horn on the titanium layer, which creates the surface profile that the aluminum tape deforms into.

Surfaces in contact with the textured horn are generally rougher than surfaces not in contact. Because in our study the layer in contact with the horn is always made of titanium, the titanium layers have a rougher topography than the aluminum layers. Hence, when the aluminum tape is placed on top, there are more significant peaks and valleys for the aluminum to flow into, causing greater mechanical interlocking at these layers. This explains the fact that builds with more bilayers exhibit much lower strengths compared with builds with fewer bilayers. In the builds with four, six, and eight bilayers, there are fewer total layers that are in contact with the horn. In turn, there are fewer layers where a large amount of mechanical interlocking could occur.

## 5 Conclusions

A DOE utilizing a Taguchi mixed array was carried out on UAM Ti/Al composites for four process parameters (normal force, amplitude, weld speed, and number of bilayers) at four levels each. Standardized methods of mechanical testing (shear and transverse tensile) were established and verified. Due to delamination during UAM or during the post-processing and machining, many of the treatment combinations could not be tested. There was great variability between all samples in both shear and tensile tests and samples mainly broke in a macro-level brittle fracture mode between layers. The greatest shear strength observed is about 68 MPa (experiment 12), which is close to the shear strength of solid 1100-O aluminum. The transverse tensile strengths are all much less than the ultimate tensile strength of both parent materials with the greatest average UTTS being 53% less than that of solid 1100-O aluminum.

Generalized linear models were used to study the dependence of USS and UTTS on the four process parameters. Bivariate models involving two of the factors at a time were investigated. In addition, linear contrasts and linear regression models were studied to further explore these relations. Larger sample sizes are needed in order to fit models with all four factors and possible interactions among them. While further studies are necessary to fully assess the effects of the parameters in this study, the trends indicate that the following combination of levels of process parameters examined in this DOE produce the highest strengths: normal force of 1500 N, oscillation amplitude of 30 $\mu$m, weld speed between 21 mm/s (50 in./min) and 42 mm/s (100 in./min), and two bilayers.

Examination of sample microstructures revealed that little to no metallurgical bonding occurred at the interface. The softer aluminum is believed to flow around the topography of the harder titanium, which in turn does not allow for deformation of asperities, thereby limiting nascent surface contact area, which is necessary for solid-state bonding. The strength of the builds is derived from the severity of the mechanical interlocking of the two metals at the interface due to the imprinting of a roughness from the horn.


## Acknowledgment

The authors would like to thank Matt Short and Karl Graff of Edison Welding Institute, Angela Dean of Ohio State University Department of Statistics, and Solidica, Inc. Financial support for this research was provided by the member organizations of the Smart Vehicle Concepts Center (www.SmartVehicleCenter.org), a National Science Foundation Industry/University Collaborative Research Center.


## References


[1] Graff, K., 2005, *New Developments in Advanced Welding*, Woodhead, Cambridge, England.

[2] Kong, C. Y., Soar, R. C., and Dickens, P. M., 2004, "Optimum Process Parameters for Ultrasonic Consolidation of 3003 Aluminium," J. Mater. Process. Technol., **146**(2), pp. 181–187.

[3] Kong, C. Y., and Soar, R. C., 2005, "Fabrication of Metal-Matrix Composites and Adaptive Composites Using Ultrasonic Consolidation Process," Mater. Sci. Eng., A, **412**(1–2), pp. 12–18.

[4] Siggard, E., 2007, "Investigative Research Into the Structural Embedding of Electrical and Mechanical Systems Using Ultrasonic Consolidation," MS thesis, Utah State University, Logan, UT.

[5] White, D. R., 2003, "Ultrasonic Consolidation of Aluminum Tooling," Adv. Mater., **161**(1), pp. 64–65.

[6] Kulakov, M., and Rack, H. J., 2009, "Control of 3003-H18 Aluminum Ultrasonic Consolidation," ASME J. Eng. Mater. Technol., **131**, p. 021006.

[7] Kong, C. Y., Soar, R. C., and Dickens, P. M., 2003, "Characterisation of Aluminium Alloy 6061 for the Ultrasonic Consolidation Process," Mater. Sci. Eng., A, **363**(1–2), pp. 99–106.

[8] Montgomery, D. C., 1991, *Design and Analysis of Experiments*, Wiley, New York.

[9] Dean, A., and Voss, D., 1999, *Design and Analysis of Experiments*, Springer, New York.

[10] SAS Institute, Inc., 2004, SAS 9.1, Cary, NC.

[11] Li, D., and Soar, R., 2009, "Influence of Sonotrode Texture on the Performance of an Ultrasonic Consolidation Machine and the Interfacial Bond Strength," J. Mater. Process. Technol., **209**, pp. 1627–1634.

[12] Yang, Y., Janaki Ram, G. D., and Stucker, B. E., 2007, "An Experimental Determination of Optimum Processing Parameters for Al/SiC Metal Matrix Composites Made Using Ultrasonic Consolidation," ASME J. Eng. Mater. Technol., **129**, pp. 538–549.

[13] Janaki Ram, G. D., Yang, Y., George, J., Robinson, C., and Stucker, B., 2006, "Improving Linear Weld Density in Ultrasonically Consolidated Parts," Proceedings of the 17th Solid Freeform Fabrication Symposium, Austin, TX.

[14] Joshi, K. C., 1971, "The Formation of Ultrasonic Bonds Between Metals," Welding Journal, **50**(12), pp. 840–848.